Available online at www.sciencedirect.com
SCIENCE DIRECT
Polymer 46 (2005) 11424–11434
polymer
www.elsevier.com/locate/polymer

Microstructural characterisation of surfactant treated nylon fibres

Stephen M. King [a,*], David G. Bucknall [b]

[a] Large Scale Structures Group, ISIS Facility, Rutherford Appleton Laboratory, Chilton, OX11 0QX, UK
[b] Polymer, Textile and Fiber Engineering, Georgia Institute of Technology, Atlanta, GA 30332-0295, USA

Received 19 September 2005; accepted 21 September 2005
Available online 11 October 2005

Abstract

Small-angle neutron scattering and differential scanning calorimetry have been used to probe for changes in the microstructure of nylon fibres following exposure to surfactant, acid and alkali solutions. SANS was also used to investigate fibres that had been subjected to intentional loading, environmental exposure, and natural ageing. A number of structural parameters have been derived. The data are capable of differentiating between untreated, treated, loaded, and used fibres. Mostly subtle effects are observed. Only exposure to concentrated acid solutions, or applied strain, imparted any significant structural perturbation. These findings, though relevant in a number of areas of application of nylon fibres, are discussed with particular reference to nylon ropes and the laundering of nylon textiles.

Keywords: Nylon; SANS; Fibre structure

1. Introduction

Nylons (polyamides) are among the most successful of the synthetic bulk commodity polymers to have emerged from the last Century. This success is largely due to the excellent fibre properties of the polymers, particularly nylon-6 (polyamide-6, polycaprolactam) and nylon-6/6 (polyamide-66). Applications for these fibres largely fall into two classes; woven (e.g. in clothing textiles, carpets, parachute 'silk', and sails) and non-woven (e.g. in tyre reinforcement cord, ropes, fishing line, sports racket and guitar 'strings', and dental floss).

Nylon fibres are often characterised as having good strength coupled with chemical resilience and low moisture absorbency. These three factors are, however, closely inter-dependent. For instance, whilst it is well known that the amide linkage (–CO–NH–) is susceptible to acid hydrolysis and UV degradation, water absorbtion can substantially reduce both the glass transition temperature and Young's modulus [1–3].

The mechanical and physical properties of nylon fibres are controlled by the response of the underlying microstructure. This is because nylons are in fact semi-crystalline polymers where finite sections of crystalline lamellae (or 'sheets') and amorphous polymer alternate throughout a 'lamellar stack' (Fig. 1). The crystallinity of a lamellar stack may be as high as 70–80%, but the overall crystallinity of a fibre is perhaps only 45–50%. A useful overview of the structural hierarchy of nylon-6 has recently been given by Rieger [4].

The crystalline lamellae are the result of hydrogen bonding between adjacent polymer chains. In the α (and β) phase of nylon-6, hydrogen bonds form between 'ribbon-like' all-trans antiparallel chains. In contrast, the γ phase of nylon-6 has a 'twisted-helical' conformation that allows hydrogen bonding to take place between neighbouring parallel chains (and the direction of the chains reverses in alternate sheets). Nylon-6/6 has analogous α and β phases (but no γ phase), but because the nylon-6/6 unit cell is centrosymmetric there is no concept of parallel and antiparallel chains, the two arrangements are equivalent.

In the case of nylon-6, fibre production has a tendency to promote the formation of the kinetically favoured γ phase over the thermodynamically stable α phase, but because melting and recrystallisation can convert $\gamma \rightarrow \alpha$ both phases are usually present in the final fibre (the ratio depending on the actual processing conditions).

There is a significant body of work on the mechanisms and molecular consequences of the hydration of nylon-6 by Murthy and co-workers [6–10] and others [11] using techniques such as SAXS, WAXS, SANS, INS, IR/Raman and ^{2}D NMR.

Understanding the structure, and how it changes, is important because has been shown that solvent molecules can diffuse into the amorphous regions (from where

* Corresponding author. Tel.: +44 1235 446437; fax: +44 1235 445720.
E-mail address: s.m.king@rl.ac.uk (S.M. King).

0032-3861/$ - see front matter © 2005 Elsevier Ltd. All rights reserved.
doi:10.1016/j.polymer.2005.09.064

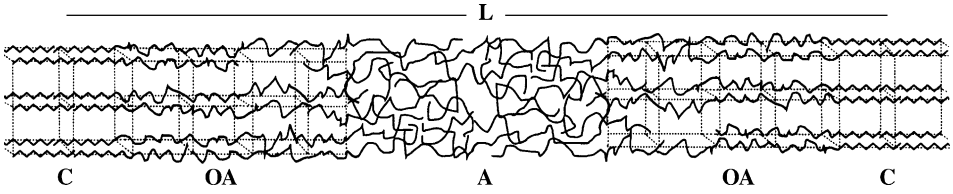

Fig. 1. Idealised schematic representation of the arrangement and different types of polymer chain conformations in a lamellar stack. Key: C, crystalline; OA, oriented amorphous, and A, amorphous polymer; *L*, Long Period. Adapted reprint from Ref. [5]. Copyright (2002), with permission from Elsevier.

a proportion of these solvent molecules also appear to diffuse between the lamellae in the crystalline regions) to replace the intercatenary hydrogen bonds [3]. This is what affects the glass transition temperature and Young's modulus. On average, one water molecule is associated with every amide (–CONH–) linkage in the amorphous regions [6]. One other, perhaps surprising, observation is that it appears as much as two-thirds of the amorphous chains lie outside of the lamellar stacks.

It is reasonable to assume that where water molecules might penetrate, so might other small molecules. Indeed, Murthy [10] compared solvation by water with that by ethylene glycol (a 'stronger' solvent). But, arguably, the molecules with the greatest potential impact on the microstructure of nylons are surfactants. This is because in several of the applications of nylon fibres it is inevitable that at some stage the fibres will be exposed to surfactant solutions for laundry/cleaning purposes. Though there are some examples relating to the adsorption of molecules like dyes and proteins/DNA, the available literature on the adsorption of surfactants by nylon is, to all intents and purposes, non-existent (one may speculate for reasons of commercial confidentiality). On the other hand, there is conflicting anecdotal evidence in, for example, the outdoor pursuits sector about the wisdom of using commercial detergent formulations and fabric conditioners on synthetic fibre ropes [12,13].

In a previous publication [14], we have reported on a preliminary study into the effects of acid, alkali and specific surfactants on the microstructure of nylon fibres. Those data, from just one fibre source, were exclusively derived from small-angle neutron scattering (SANS) measurements. In this contribution we additionally report new SANS measurements: (a) on fibres from a second sample source, (b) on 'real-life' and 'deliberately aged' samples, and (c) on samples under load. We also report on some ancillary calorimetric measurements on the original samples.

2. Experimental

For more comprehensive experimental details see King [14].

2.1. Materials

Deuterium oxide (D_2O), sodium deuteroxide (NaOD), perdeuterated sulphuric acid (D_2SO_4), and perdeuterated sodium dodecyl (or lauryl) sulphate (dSDS) were obtained from the Aldrich Chemical Co. Ltd. Perdeuterated hexadecyl (or cetyl) trimethyl-ammonium bromide ($dC_{16}TAB$) and perdeuterated hexaethyleneglycol mono-dodecyl ether (or 6 lauryl ether) ($dC_{12}E_6$) were obtained as gifts from Unilever Research. Cationic and non-ionic surfactants are the major constituents (typically 10–20%) of commercial washing powders and fabric conditioners. Anionic surfactants are sometimes also present.

Yarns of fibres approximately 3 cm in length were extracted from the cores of metre lengths of Edelrid Superstatic® static (two separate lengths, denoted here 'I' and 'II') and dynamic kernmantel rope. These ropes had previously been soaked in pure water for 10 days (to remove the sizing used in manufacture) and then dried at room temperature whilst hanging under their own weight for a further 8 days.

Fibres from Static-I samples were variously treated with solutions of acid (at 11 or 33 wt%), alkali (at 40 wt%) or surfactants (at a concentration 13 times the respective critical micelle concentration) in D_2O. These are the samples discussed previously [14].

Two sets of fibres from Static-II samples were subjected to a number of wash cycles in a domestic washing machine, including exposure to the usual amounts of household laundry powder and fabric conditioner on each occasion. One sample received 15 wash cycles (14 at 60 °C, 1 at 30 °C), the other received 62 wash cycles (38 at 60 °C, 9 at 50 °C, 14 at 40 °C, 1 at 30 °C). Both samples also received one (accidental) drying cycle of around 30 min duration.

Finally, fibres from two samples of 'used' dynamic rope, one at least 25 years old the other at least 18 years old (donated by a climber), and a sample of 'used' static rope, of unknown type and vintage—but said to be 'old'—(donated by a caver), were also investigated.

2.2. Techniques

Small- and wide-angle neutron diffraction data were measured with two-dimensional position sensitive detectors on the LOQ [15] instrument at the ISIS Spallation Neutron Source, Chilton, Oxfordshire, UK [16] in the Q-range 0.06–14 nm^{-1} (where Q is the modulus of the scattering vector). The wet fibres were clamped at each end above a small dish of D_2O inside a box with aluminium foil beam entry/exit windows (to maintain relative humidity) with their long axis vertical. The clamps also permitted an extensional strain to be applied if desired. The incident beam was collimated as a rectangular slit 8 mm (H)×2 mm (W) to match the orientation of the fibres in the beam. Each raw scattering dataset was corrected for the sample transmission and background scattering, detector efficiency and linearity, and converted to scattering

cross-section data ($\partial\Sigma/\partial\Omega$ versus Q) using the instrument-specific software [17]. This reduced data was placed on an absolute scale using a well-characterized solid blend of hydrogenous and perdeuterated polystyrene as a calibration standard [18]. The neutron scattering length densities of crystalline and amorphous nylon-6 are $+0.91\times10^{10}\,\mathrm{cm}^{-2}$ and $+0.80\times10^{10}\,\mathrm{cm}^{-2}$, respectively [7]. To a very good approximation the scattering length densities of nylon-6 and nylon-6/6 are the same.

Differential scanning calorimetery (DSC) data were obtained using a Perkin–Elmer Series 7 Thermal Analysis System. Typically, between 3 and 15 mg of sample were used, contained in closed aluminium DSC pans. The heating rate was 10 °C/min.

Wide-angle X-ray diffraction data were collected on a Siemens D5000 laboratory X-ray diffractometer (Cu K_α at 0.154 nm, 30 mA, 40 kV, bent crystal graphite monochromator) equipped with a single scintillator detector and operating in standard three-circle geometry. The X-ray beam was collimated with 2 mm slits either side of the sample position and the acceptance angle of the detector was defined by a 0.2 mm slit.

2.3. Data analysis

A sample with a narrowly-distributed quasi-regular spacing is likely to fulfil the conditions for Bragg diffraction giving rise to a 'peak' in the scattering data. The reciprocal space position of this peak can be used to estimate the Long Period, L, of the spacing through the relationship.

$$L = \frac{2\pi}{Q} = \frac{\lambda}{2\sin\theta} \tag{1}$$

where λ is the wavelength and 2θ is the scattering angle. The width of the peak is directly related to the distribution of L values. We have used the academic shareware program XFIT [19] to locate peak positions.

An alternative approach is to use the scattering data to calculate the density correlation function. In doing so it is necessary to recognise that on the length scales being probed the spacings in the lamellar stack are ordered along one axis, even though the macroscopic alignment of the fibres means that the stacks themselves are oriented over a range of angles [20]. In such instances it is necessary to compute the one-dimensional density correlation function[1], $\Gamma_1(z)$, given by [21]

$$\Gamma_1(z) = \frac{\int_0^\infty \frac{\mathrm{d}\Sigma}{\mathrm{d}\Omega}(Q)Q^2\cos(Qz)\mathrm{d}Q}{\int_0^\infty \frac{\mathrm{d}\Sigma}{\mathrm{d}\Omega}(Q)Q^2\mathrm{d}Q} \tag{2}$$

We have used the academic shareware program CORFUNC [19] to compute, and to extract structural parameters from, the resulting $\Gamma_1(z)$ functions. In applying Eq. (2), we have limited the range of azimuthal angles included in the calculation of the scattering cross-section data to sectors encompassing the dominant features of the scattering pattern.

Note that the denominator in Eq. (2) is the same as the so-called invariant integral, often denoted Q^*. This contains information about the composition of, and scattering length density difference between, the different phases. Given the length scales being investigated in this work, and the fact that the underlying surface scattering has been subtracted, the lamellar stacks can be treated as being just two-phase; crystalline polymer ('c') and hydrated amorphous polymer ('a'). Thus we may write [22]

$$\begin{aligned} Q^* &= 2\pi^2\left(\rho_\mathrm{c} - \rho_\mathrm{a}^\mathrm{eff}\right)^2 \phi_\mathrm{stacks}\omega_\mathrm{c}(1-\omega_\mathrm{c}) \\ &= 2\pi^2\left(\rho_\mathrm{c} - \rho_\mathrm{a}^\mathrm{eff}\right)^2 \phi_\mathrm{c}(1-\omega_\mathrm{c}) \end{aligned} \tag{3}$$

where ρ is the scattering length density, ω_c is termed the local crystallinity, and ϕ_c is the volume or bulk crystallinity. These last two parameters are obtained from $\Gamma_1(z)$.

The effective scattering length of the hydrated amorphous polymer can then be used to estimate the volume fraction of solvent, ϕ_sol, present since

$$\rho_\mathrm{a}^\mathrm{eff} = (1-\phi_\mathrm{sol})\rho_\mathrm{a} + \phi_\mathrm{sol}\rho_\mathrm{sol} \tag{4}$$

The integrated azimuthal intensity distribution can be used to estimate the fraction of oriented polymer chains, ϕ_orient, within a fibre sample [5,23]. This (admittedly crude) approach assumes that all the intensity in a 'peak' in such a distribution is superimposed on some baseline 'amorphous halo' value (taken as the bottom of the lowest 'trough' in each case), and arises only from the oriented chains (both crystalline and amorphous). Hence one may write (assuming a constant angular step in the summations)

$$\phi_\mathrm{orient} = \frac{\sum_0^{360^\circ}\{\mathrm{Intensity} - \mathrm{Baseline}\}}{\sum_0^{360^\circ}\{\mathrm{Intensity}\}} \tag{5}$$

from which it follows that

$$\phi_\mathrm{amorph} \approx 1 - \phi_\mathrm{orient} \tag{6}$$

3. Results and discussion

To begin, it is instructive to consider the representative radially-averaged SANS data shown in Fig. 2. Several features are apparent. At very low-Q there is quite intense scattering that decays rapidly with increasing Q. This scattering has a fractal law dependence of $\sim Q^{-3.9}$ and is attributed to surface scattering from the fibrils. This background was subtracted before any further analysis was performed.

Superimposed on the power law decay is a broad diffraction peak centred on $Q\sim0.76\,\mathrm{nm}^{-1}$ ($L\sim8.3$ nm) corresponding to the separation of the deuterium-deficient crystalline and deuterium-rich amorphous regions in the lamellar stacks [6,11]; i.e. there is a regularly repeating

[1] Were the spacings to occur in all three directions it would then be necessary to compute the *three-dimensional* function.

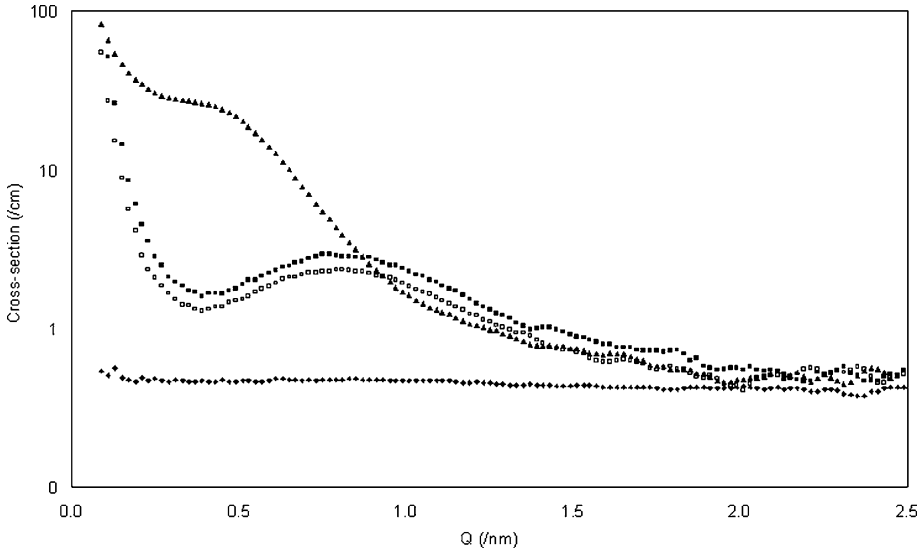

Fig. 2. The small-angle neutron scattering from fibres treated with: (■) D_2O, (□) 11 wt% D_2SO_4, and (▲) 33 wt% D_2SO_4. Also shown for comparison (cross-section×0.5) is the scattering from the same fibres but hydrated with 'contrast match water' (♦).

pattern of low and high neutron scattering length density in each stack. When this contrast difference is negligible, as in dry fibres or fibres hydrated in 'contrast match' water (a mixture 21.8 wt% D_2O: 78.2 wt% H_2O with $\rho \sim 0.85 \times 10^{10}$ cm^{-2}), the Bragg peak all but disappears. The width of the peak clearly reflects a broad distribution of repeat distances within the lamellar stacks. Thus the crystalline and amorphous regions are not all of the same length, and neither are the stacks (fibrils).

The scattering from fibres exposed to the 33 wt% D_2SO_4 solution is rather different. The Long Period has increased by such a large extent that the diffraction peak is now a shoulder on the low-Q decay. This is completely different behaviour to that exhibited by any other sample, even that treated with 11 wt% D_2SO_4. This should not though be too surprising since, on the evidence of visual inspection, the fibres in this sample had been rather seriously degraded, but it is nonetheless reassuring to see that such changes are reflected in the scattering.

Crystalline reflections are unfortunately just beyond the detection limit of the LOQ instrument (Tables 1 and 2), but are accessible to wide-angle X-ray scattering (WAXS), see Fig. 3.

Though factors such as sample age, temperature, chemical treatment and degree of hydration have all been shown to bring about subtle changes in crystallographic spacing, the diffraction peaks in the WAXS data may in principle be used to index the crystal phases. For example, from Table 1 it is readily apparent that fibres from the used dynamic (25 year vintage) rope sample are not formed from the γ-form of nylon-6 (in keeping with the earlier discussion about the relative stabilities of the γ versus α phases), but the data in Fig. 3 are not of sufficiently high resolution to be able to differentiate between the α-forms of nylon-6 and nylon-6/6.

To extract Long Period data for the different samples the Bragg (diffraction) peaks in the SANS data were fitted to a Cauchy function. The Bragg peaks in the data from fibres hydrated with H_2O, or from dry fibres, were too weak to be fitted with any reliability. The Long Period data are given in Table 3.

Table 1
Characteristic d-spacings and positions of diffraction peaks for the α and γ phases of nylon-6

Peak	d (nm)	Q (nm^{-1})	2θ (°)
α Phase			
020	Weak		
040+210	0.437	14.38	20.30
200	0.422	14.89	21.03
	0.444	14.15	19.97
	0.417	*15.07*	*21.29*
002+202	0.370	16.98	24.02
	0.371	16.94	23.96
	0.397	*15.83*	*22.37*
γ phase			
020	0.80	7.82	11.00
040+210			
001	0.403	15.59	22.03
	0.413	15.21	21.49
200+$\bar{2}$01	0.386	16.28	23.02
	0.399	15.75	22.26

Those for the high-temperature α′ phase are in italics. The 200+$\bar{2}$01 reflections appear as a shoulder to the 001 reflection. Data taken from Refs. [24,25].

Table 2
Characteristic d-spacings and positions of diffraction peaks for the α phase of nylon-6/6

Peak	d (nm)	Q (nm^{-1})	2θ (°)
α Phase			
100	0.437	14.36	20.27
010+110	0.372	16.87	23.86

Data taken from Ref. [26].

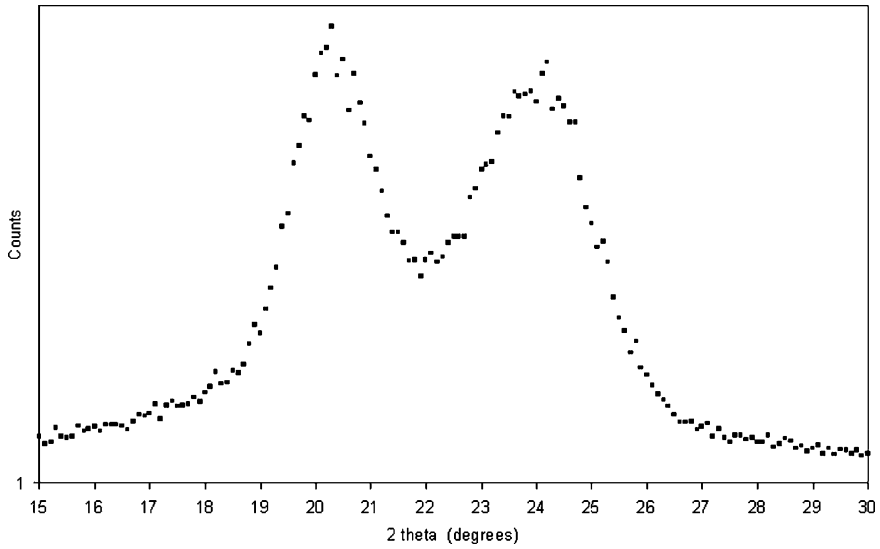

Fig. 3. The wide-angle X-ray scattering from fibres of the used dynamic (25 year vintage) sample.

Excluding the data for fibres treated with 33 wt% D_2SO_4, the average spacing for the Static-I samples is 8.41 ± 0.45 nm. This compares exceptionally well with a literature value of 8.4 nm for unannealed nylon-6 films treated with D_2O [6]. Including the unstrained Static-II samples and the Used Static sample only changes the average spacing to 8.34 ± 0.42 nm. Just five of the 14 values spread across three different sources of fibres lie outside one standard deviation, and there is no obvious trend to the outliers.

Table 3
Summary of the structural data derived from peak fitting analysis

Treatment	Comment	L (nm)	ΔQ (nm^{-1})
Static-I			
D2O		8.61	0.71
dSDS		8.73	0.67
dSDS	After 41 months	7.76	0.74
$dC_{16}TAB$		8.98	0.85
$dC_{12}E_6$		8.38	0.68
$dC_{12}E_6$	After 41 months	8.17	0.54
NaOD		8.06	0.65
NaOD	After 41 months	7.80	0.81
11% D_2SO_4		8.61	0.66
11% D_2SO_4	After 41 months	9.00	0.53
33% D_2SO_4		21.7	0.42
Static-II			
D_2O		7.72	0.72
D_2O	50% Extension	8.62	0.56
D_2O	15 Washes	8.27	0.60
D_2O	62 Washes	8.46	0.60
Dynamic			
D_2O	0% Extension	9.75	0.60
D_2O	50% Extension	11.1	0.76
D_2O	100% Extension	10.8	0.76
Used			
D_2O	Static (?? years)	8.26	0.79
D_2O	Dynamic (18 years)	9.09	0.55
D_2O	Dynamic (25 years)	10.3	0.71

Key: L, Long Period; ΔQ, peak width (FWHM).

Comparing the change in Long Period with applied strain for the static-II and dynamic samples immediately shows a change in excess of two standard deviations and, reassuringly, the change is bigger in the dynamic sample (designed to be more 'elastic') than it is in the static-II sample for the same extension. From these observations we conclude: (1) that mechanically straining the fibres perturbs the microstructure to a much greater degree than (even quite extended) exposure to surfactants, alkali or dilute acid, and (2) that the effects of the chosen chemical treatments (excepting the 33 wt% D_2SO_4 data) are indistinguishable from the natural sample-to-sample variability of the fibres.

Despite this there are some trends in the data. Prolonged exposure to concentrated surfactant or alkali solutions appears to bring about a reduction in L, the effect being most pronounced for the anionic surfactant SDS and least pronounced for the non-ionic $C_{12}E_6$ (though there was insufficient $dC_{16}TAB$ for us to include this in the long-term studies). Exposing the fibres to concentrated acid solutions, or to dilute acid solutions for an extended period, or straining the fibres, increases L. This is, of course, in keeping with the known degradation behaviour of polyamides and the expected effects of mechanical deformation. But extensive laundering also seems to increase the spacing, by amounts comparable to what may be achieved by moderate loading of the fibres. When viewed in the light of the data from the 'quiescent' surfactant-treated samples this is a finding that should perhaps be subject to more investigation.

Interestingly, the average spacing in the dynamic and used dynamic samples appears to be slightly larger, 9.71 ± 0.60 nm, than in the static samples. This most likely reflects the use of a polymer other than nylon-6, or a blended product.

Comparing the data for the used samples with the data for the various new untreated, unstrained, samples suggests

that if long-term 'natural' ageing has an effect on the microstructure it is quite small (since the values of L are almost within one standard deviation of the average values given above).

The correlation functions for the samples reported in Table 3 are shown in Fig. 4, and give a clear indication of what the variability between samples and the effects of treatments and aging is like. The structural parameters derived from the correlation functions are given in Tables 4 and 5.

Comparing first the Long Period data in Tables 3 and 4, it will be observed that the values of L derived by correlation function analysis are consistently smaller than those derived from the earlier peak fitting analysis. In the case of the static samples (this time also excluding the used static sample) the average spacing from Table 4 works out at 6.33 ± 0.48 nm, whilst that for the dynamic and used dynamic samples is 7.27 ± 0.49 nm. Both values represent a reduction of about 25% on the figures derived from peak fitting. This probably arises because correlation function analysis assumes that the fibre microstructure possesses an ideal lamellar morphology [21]. This is, of course, not the case, as shown in Fig. 1. The oriented amorphous polymer will tend to 'blur' the lamellar boundary. Though other 'dimensional' parameters, such as the average thicknesses of the crystalline or amorphous regions, will be similarly affected, trends and parameters based on ratios, such as the crystallinity, should be internally consistent. It is reassuring therefore, that the same statistical outliers are observed in Table 4 as were identified in Table 3, and once again the Long Period in strained samples lies more than two standard deviations from the average value. The data in Table 4 also reinforce the conclusions drawn earlier about the effects of concentrated surfactant and alkali solutions, dilute acid solutions, laundering, mechanical deformation and ageing.

The average thickness of the crystalline (l_c) and amorphous (l_a) regions in the unstrained, unlaundered, Static samples is 1.30 ± 0.22 nm (for comparison the c-dimension

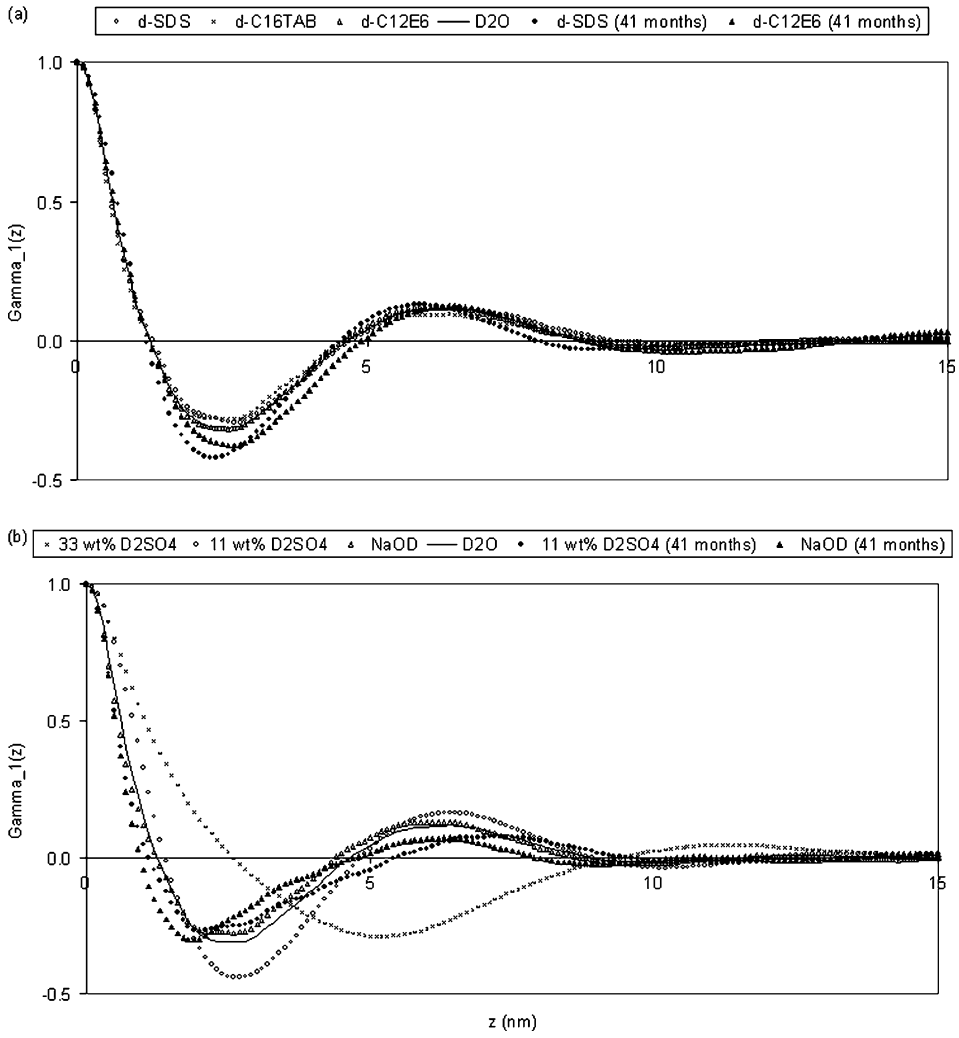

Fig. 4. The correlation functions calculated from the 1D small-angle scattering data such as that shown in Fig. 2. (a) Static-I samples hydrated with D_2O and surfactant solutions. (b) Static-I samples hydrated with acid and alkali solutions. (c) Static samples hydrated with D_2O. (d) Dynamic samples hydrated with D_2O.

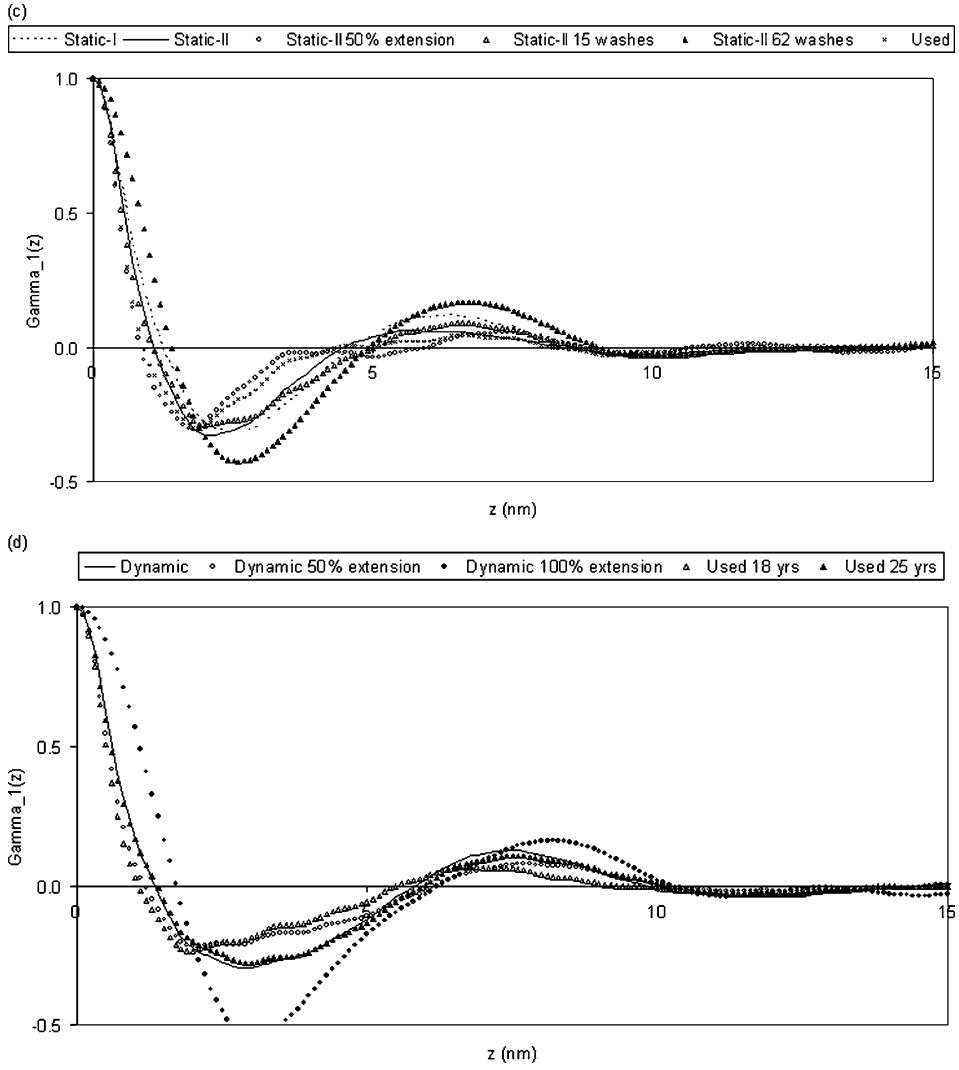

Fig. 4 (*continued*)

of the monoclinic unit cell of nylon-6 is ~1.72 nm) and 4.82±0.67 nm, respectively. And from Table 5 the average degree of crystallinity of these fibres is 21±2%. For comparison the equivalent figures for the unstrained dynamic samples are 1.24±0.18 nm, 6.02±0.34 nm, and 18±2%, respectively; i.e. fibres in the dynamic samples are less crystalline, which seems sensible. Straining the fibres to 50% extension reduces l_c, increases l_a, and reduces the apparent crystallinity, but this effect is reversed at higher extensions. The effect of progressive laundering appears to be broadly similar. There are some obvious parallels here with basis of rubber elasticity, the stretching of topological networks, and 'strain-hardening'.

Murthy [27] has proposed that an increase in the crystallinity could arise through an increase in the ordering of the oriented amorphous chains in the lamellar stack, and vice versa. To investigate this we have followed the procedure of Wu and Schultz [5] outlined earlier. The 2D small-angle diffraction patterns from the fibres are actually anisotropic, as shown in Fig. 5 for example. When the integrated intensity in the Bragg peak is plotted against azimuthal angle a distinct four-peak pattern emerges as shown in Fig. 6.

This data was used to calculate the fraction of oriented polymer in the fibres, ϕ_{orient} shown in Table 6. The four peaks are evidence of biaxial alignment of the nylon chains in the fibres, imparted during the manufacturing process [28]. Note that as the fibres are subjected to increasing strain the Bragg peak and the four-peak pattern both become much better defined. The apparent loss of intensity at high strain is probably due to a loss of contrast as D_2O is squeezed out. Certainly, there is a marked reduction in the volume fraction of solvent in the amorphous regions with applied strain in these samples, see Table 5.

Interestingly, fibres treated with concentrated acid and alkali only exhibit two-peak patterns, aligned along the equator [14]. This suggests a loss of register between chains in the direction across the fibres.

In the case of strained fibres the Murthy hypothesis appears to be borne out; the fraction of oriented polymer, see Table 6,

Table 4
Summary of the structural data derived from correlation function analysis

Treatment	Comment	L (nm)	l_c (nm)	l_a (nm)
Static-I				
D_2O		6.50	1.31	5.18
dSDS		6.50	1.32	5.17
dSDS	After 41 months	5.90	1.52	4.37
$dC_{16}TAB$		5.80	1.26	4.53
$dC_{12}E_6$		6.30	1.31	4.98
$dC_{12}E_6$	After 41 months	6.50	1.45	5.04
NaOD		5.80	1.24	4.55
NaOD	After 41 months	6.40	1.06	5.33
11% D_2SO_4		6.40	1.81	4.58
11% D_2SO_4	After 41 months	7.40	1.16	6.24
33% D_2SO_4		11.4	2.56	8.83
Static-II				
D_2O		5.60	1.23	4.37
D_2O	50% Extension	7.50	0.96	6.53
D_2O	15 Washes	6.60	1.11	5.49
D_2O	62 Washes	6.70	1.81	4.89
Dynamic				
D_2O	0% Extension	7.50	1.40	6.10
D_2O	50% Extension	7.70	1.11	6.59
D_2O	100% Extension	8.20	2.50	5.69
Used				
D_2O	Static (?? years)	4.50	0.99	3.50
D_2O	Dynamic (18 years)	6.70	1.04	5.65
D_2O	Dynamic (25 years)	7.60	1.28	6.32

Key: L, Long Period; l_c, average thickness of crystalline region; l_a, average thickness of amorphous region.

Table 5
Summary of the physical data derived from correlation function and invariant analysis

Treatment	Comment	ϕ_c	ω_c	ϕ_{sol}
Static-I				
D_2O		0.21	0.20	0.69
dSDS		0.20	0.20	0.62
dSDS	After 41 months	0.25	0.26	0.25
$dC_{16}TAB$		0.20	0.22	0.72
$dC_{12}E_6$		0.21	0.21	>1
$dC_{12}E_6$	After 41 months	0.24	0.22	0.19
NaOD		0.19	0.21	0.34
NaOD	After 41 months	0.20	0.17	0.27
11% D_2SO_4		0.26	0.28	0.53
11% D_2SO_4	After 41 months	0.19	0.16	0.52
33% D_2SO_4		0.21	0.22	n/a
Static-II				
D_2O		0.21	0.22	0.27
D_2O	50% Extension	0.20	0.13	0.27
D_2O	15 Washes	0.20	0.17	0.30
D_2O	62 Washes	0.25	0.27	0.33
Dynamic				
D_2O	0% Extension	0.21	0.19	0.47
D_2O	50% Extension	0.15	0.14	0.51
D_2O	100% Extension	0.29	0.30	0.27
Used				
D_2O	Static (?? years)	0.20	0.22	0.35
D_2O	Dynamic (18 years)	0.16	0.16	0.51
D_2O	Dynamic (25 years)	0.19	0.17	0.38

Key: ϕ_c, volume crystallinity; ω_c, local crystallinity (l_c/L); ϕ_{sol}, volume fraction of solvent in amorphous regions.

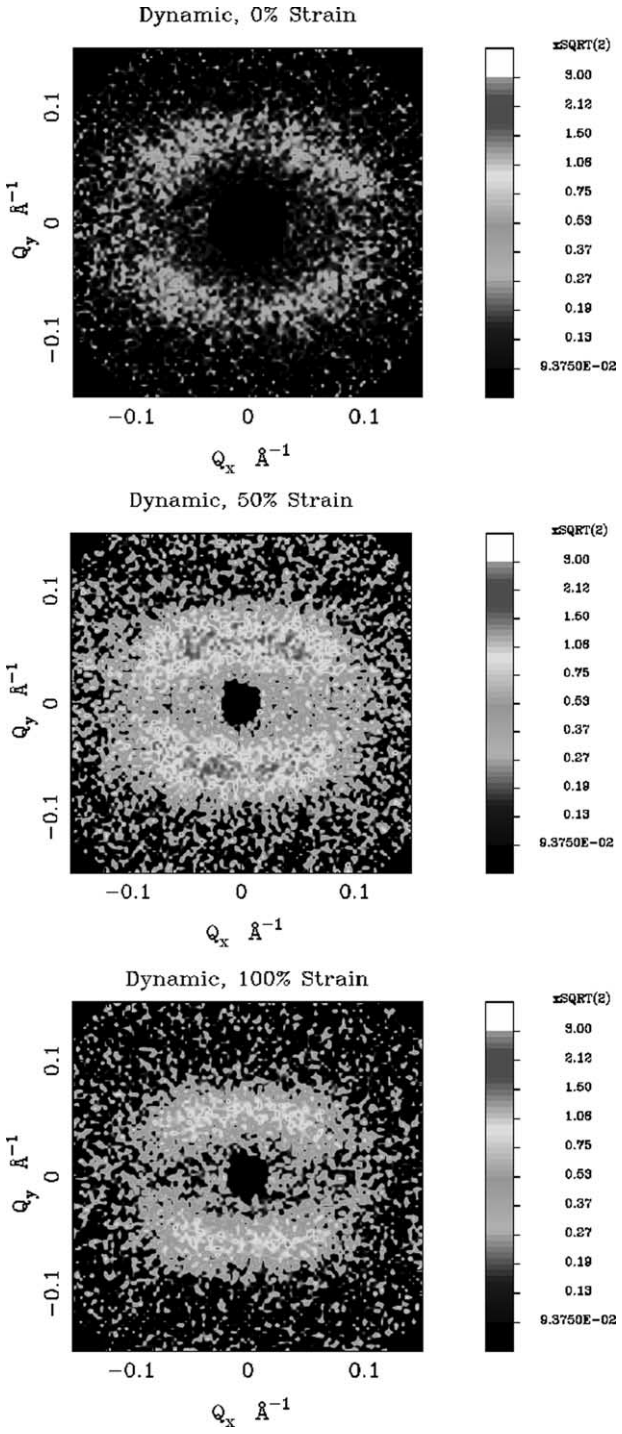

Fig. 5. The 2D small-angle scattering (to the same intensity scale) from dynamic fibres hydrated with D_2O, (top) 0% strain, (middle) 50% strain, (bottom) 100% strain.

rises from about 58–66% for the static samples, and from about 23–49% for the dynamic sample at 50% extension (rising further to 59% in the dynamic sample at 100% extension). However, different behaviour is observed in the laundered samples and those samples exposed to dSDS, alkali or dilute acid for an extended period. In these cases ϕ_{orient} is actually smaller (and ϕ_{amorph} is larger) than in the untreated, unstrained, unlaundered static samples, even though the apparent

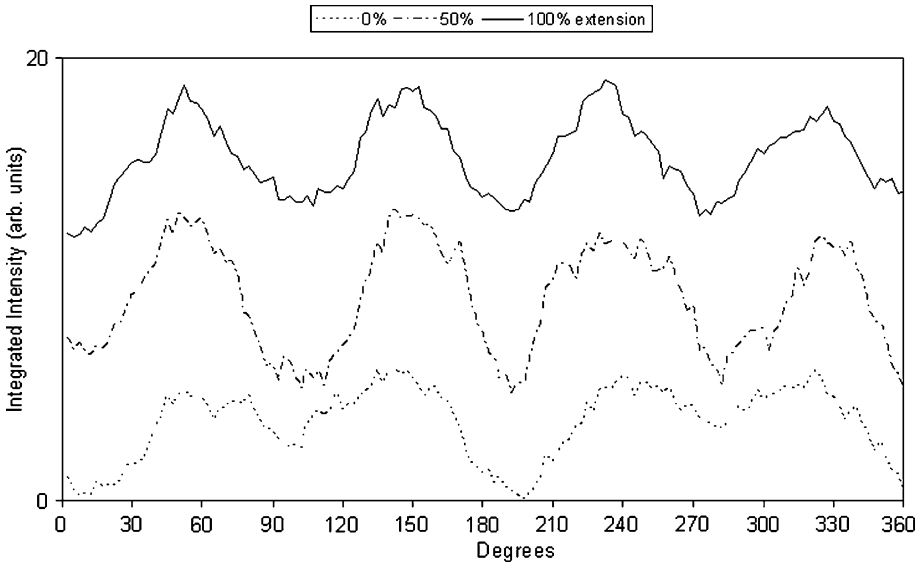

Fig. 6. The (exponentially smoothed) integrated azimuthal intensity in the Bragg peak from dynamic fibres hydrated with D_2O under strain. The data is that shown in Fig. 5. The curves have been displaced vertically to aid clarity. The equator of the 2D scattering pattern is represented by 0 and 180°.

crystallinity is broadly similar. This seeming contradiction could be explained by the presence of a smaller fraction of oriented amorphous polymer in these samples (assuming the crystallinity only reflects the fraction of truly oriented chains by virtue of the ideal lamellar morphology). It is then interesting to note that the used static sample has the smallest value of ϕ_{orient} of any of the Static samples. On the other hand, ageing does not appear to have similarly affected the used dynamic samples. However, the detailed histories of the used samples are unknown, and the ageing processes that might affect the two types of used sample are likely to have been rather different [29].

Table 6
Summary of the fraction of oriented and amorphous polymer in the fibres derived from the integrated intensity plots in Fig. 6

Treatment	Comment	ϕ_{orient}	ϕ_{amorph}
Static-I			
D_2O		0.60	0.40
dSDS		0.63	0.37
dSDS	After 41 months	0.51	0.49
$dC_{16}TAB$		0.54	0.46
$dC_{12}E_6$		0.59	0.41
$dC_{12}E_6$	After 41 months	~1	~0
NaOD		0.65	0.35
NaOD	After 41 months	0.38	0.62
11% D_2SO_4		0.59	0.41
11% D_2SO_4	After 41 months	0.40	0.60
33% D_2SO_4		0.30	0.70
Static-II			
D_2O		0.54	0.46
D_2O	50% Extension	0.66	0.34
D_2O	15 Washes	0.31	0.69
D_2O	62 Washes	0.42	0.58
Dynamic			
D_2O	0% Extension	0.23	0.77
D_2O	50% Extension	0.49	0.51
D_2O	100% Extension	0.59	0.41
Used ropes			
D_2O	Static (?? years)	0.22	0.78
D_2O	Dynamic (18 years)	0.29	0.71
D_2O	Dynamic (25 years)	0.23	0.77

Key: ϕ_{orient}, all oriented polymer; ϕ_{amorph}, amorphous polymer only.

Supplementary DSC measurements show (Fig. 7) that none of the surfactants affect the melting temperature, T_m, of the fibres (circa 223 °C from the data for the 'dry', untreated, sample). The endotherm evident in the dSDS trace at 183 °C may be due to residual and/or partially-hydrolysed surfactant ($T_{m,dSDS} \sim 199$ °C) crystallised on the fibres.

The DSC data for those fibres exposed to NaOD and D_2SO_4 are rather more interesting. The NaOD trace still shows the nylon T_m endotherm but also shows a much larger endotherm some 60 °C lower in temperature. The nylon T_m endotherm appears absent in the D_2SO_4 data, but is replaced by one approximately 40 °C lower. None of the endotherms in these DSC traces correlate with the melting or boiling points of NaOD or D_2SO_4 and so are presumed to reflect a change in the microstructure of the polymer. This would tie in with the observed differences in the azimuthal intensity distribution. Both effects could be the result of disruption to the inter-chain hydrogen-bonding.

Between the start of the DSC traces and the onset of melting there is a broad exotherm (manifested in the curvature of the trace). This is due in part to what is termed 'cold' or 'silent' (but is nonetheless heat-activated) crystallisation and which must be corrected for when using DSC to determine the crystallinity of nylon-6, and in part to the endothermic loss of moisture [30,31].

At temperatures <50 °C weak exotherms are evident. These are believed to be associated with the glass transition, T_g, of the polymer. Determinations of T_g were made by graphical extrapolation and are summarised in Table 7. No determinations were made from the data of fibres exposed to NaOD because the relevant region of the DSC trace contains a number of irregular peaks (just visible in Fig. 7(b)). This was the only sample to exhibit such behaviour.

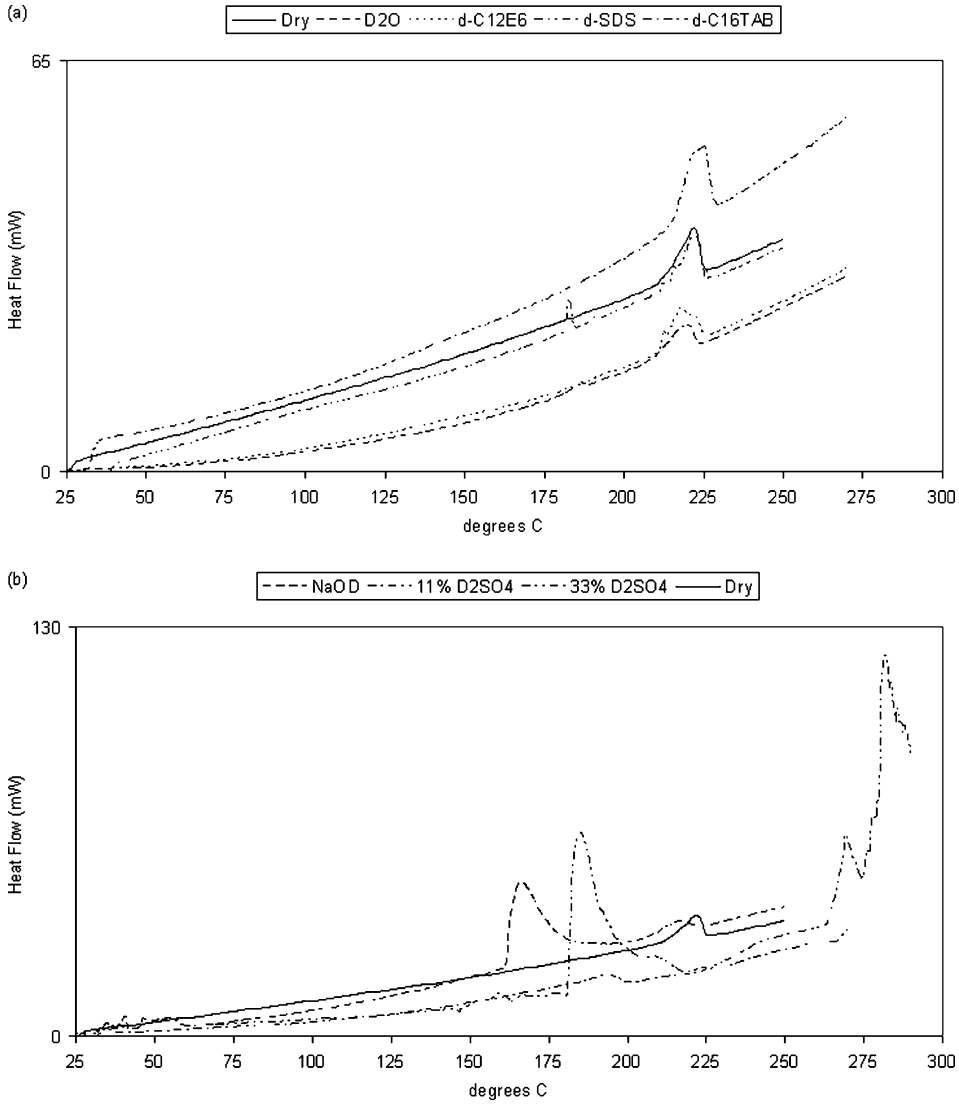

Fig. 7. DSC data from treated static-I fibre samples. Key: (a) D_2O and surfactant solutions. (b) Acid and alkali solutions.

The T_g estimates in Table 7 are all lower than the 'literature' values, 47–57 °C for nylon-6 and 35–78 °C for nylon-6/6, but as has already been discussed (see for example Fig. 2 in Ref. [14]) the glass transition in nylon-6 (and polyamides in general) is notoriously sensitive to the degree of hydration.

Table 7
T_g data for static-I samples derived from DSC measurements

Treatment	$T_{g,peak}$ (°C)	$T_{g,iflx}$ (°C)
None	25.3	26.5
D_2O	25.7	27.0
dSDS	36.9	38.0
$dC_{16}TAB$	31.0	32.5
$dC_{12}E_6$	25.9	27.5
NaOD	–	–
11% D_2SO_4	30.2	31.3
33% D_2SO_4	<25	<26

Key: $T_{g,peak}$, position of the exotherm peak (±0.1 °C); $T_{g,iflx}$, position of the inflexion point on the DSC trace on the high-temperature side of the exotherm peak (±0.5 °C).

4. Conclusion

Small-angle neutron scattering (SANS) and differential scanning calorimetry (DSC) have been used to probe for changes in the microstructure of nylon fibres following exposure to surfactant, acid and alkali solutions. SANS was also used to investigate fibres that had been subjected to intentional loading and environmental exposure. The data are capable of differentiating between untreated, treated, loaded, and used fibres.

There are three principal conclusions to be drawn from the data. First, compared to those fibres that have simply been hydrated with water, and excepting the effects of exposure to concentrated acid solutions, none of the chosen chemical treatments alone appear to bring about any gross microstructural changes. However, applying a mechanical strain to the fibres perturbs the microstructure to a much greater degree than even quite extended exposure to solutions of surfactants, alkali or dilute acid. And finally, if long-term 'natural ageing' has an effect on the microstructure it appears to be quite a small effect.

These conclusions are interesting because they mirror those drawn from mechanical testing. Smith [12] found that treating nylon rope with concentrated fabric conditioner reduced the tensile strength (breaking load) in dynamic tests. And the degree of deterioration increased with the age or use of the rope. But Frank [13] showed that ropes treated with dilute fabric conditioner (as per the manufacturer's instructions) were in fact stronger than the same rope without conditioning, after ageing and wear. Frank's explanation was that the manufacturing lubricants present in new rope are gradually lost with age and use, allowing the fibres to 'cut' into one another (thereby reducing the fibre redundancy that contributes to the load handling capability of the rope). Frank suggested that the addition of fabric conditioner can offset some of this loss of lubrication, but excess quantities effectively leave the rope fibres wet, with a corresponding loss in strength [1–3]. There are some indications in our data that cationic surfactants are more effective at keeping the amorphous regions hydrated than either anionic or non-ionic surfactants. Indeed this may be one of the reasons why cationics constitute the bulk of the surfactants present in commercial laundry detergents and fabric conditioners.

The above notwithstanding, careful analysis of the data reveals that prolonged exposure of nylon fibres to concentrated surfactant or alkali solutions brings about a small reduction in the Long Period of the lamellar stacks. Whereas exposing the fibres to concentrated acid solutions, or to dilute acid solutions for an extended period, or straining the fibres, appears to increase the Long Period. Extensive laundering also seems to increase the spacing, by amounts comparable to what may be achieved by the application of moderate strains to the fibres.

The effect of straining untreated fibres appears to be a two stage process. Initially, at low strains, the lamellar stacks become 'more amorphous', but at high strains they become 'more crystalline'. This behaviour is likely to be the result of progressive changes in the ordering of oriented amorphous polymer. In unstrained fibres exposed to alkali, or to dilute acid for an extended period, there appears to be a smaller proportion of oriented amorphous polymer overall. This is thought to be related to subtle changes in the hydrogen-bonding network in these samples, but requires further investigation.

It should be possible to adapt the methodology used here to investigate other fibres of commercial importance.

Acknowledgements

The authors wish to thank: Dr Ian Tucker (Unilever Research, UK) for providing the $dC_{16}TAB$ and $dC_{12}E_6$ surfactants; Mr Andrew Manthorpe (Swindon Mountaineering Club, UK) for donating the Used Dynamic rope; Dr Christopher Densham (Oxford University Caving Club, UK) for donating the Used Static rope; Mr Phillip Taylor and Dr Timothy Charlton (ISIS, UK) for making the WAXS measurements; Mr Lewis Morgan (Oxford University, UK) for assistance with the DSC measurements, and Mr William Boehle (Secretary, NSS Vertical Section) for providing copies of Refs. [12,13].

References

[1] Kaimin IF, Apinis AP, Aya G. Vysokomol Soedin 1975;A17:41.
[2] Inoue K, Hoshino S. J Polym Sci, Polym Phys Ed 1976;14:1513.
[3] Reimschuessel HK. J Polym Sci, Polym Chem Ed 1978;16:1229.
[4] Rieger J. In: Lindner P, Zemb Th, editors. Neutrons X-rays and light: scattering methods applied to soft condensed matter. NY, USA: North-Holland; 2002 [chapter 21].
[5] Wu J, Schultz JM. Polymer 2002;43:6695.
[6] Murthy NS, Stamm M, Sibilia JP, Krimm S. Macromolecules 1989;22:1261.
[7] Murthy NS, Orts WJ. J Polym Sci, Part B 1994;32:2695.
[8] Papanek P, Fischer JE, Murthy NS. Macromolecules 2002;35:4715.
[9] Hutchinson JL, Murthy NS, Samulski ET. Macromolecules 1996;29:5551.
[10] Murthy NS, Akkapeddi MK, Orts WJ. Macromolecules 1998;31:142.
[11] Plestil J, Baldrian J, Ostanevich YuM, Bezzabotnov VY. J Polym Sci, Part B 1991;29:509.
[12] Smith B. Nylon Highway 1988;25.
[13] Frank JA. Nylon highway 1989;28.
[14] King SM, Bucknall DG, Heenan RK. Fibre Diffr Rev 2004;12:41 [www.fibrediffractionreview.org].
[15] (a) www.isis.rl.ac.uk/LargeScale/LOQ/LOQ.htm.
(b) King SM. Fibre Diffr Rev 2004;12:15 [www.fibrediffractionreview.org].
[16] www.isis.rl.ac.uk.
[17] King SM, Heenan RK. RAL Report RAL-95-005. Rutherford Appleton Laboratory; 1995.
[18] Wignall GD, Bates FS. J Appl Cryst 1987;20:28.
[19] www.ccp13.ac.uk.
[20] Ryan AJ. Fibre Diffr Rev (www.fibrediffractionreview.org) 19944;3:25.
[21] Strobl GR, Schneider M. J Polym Sci, Polym Phys Ed 1980;18:1343.
[22] Li L, Koch MH, de Jeu WH. Macromolecules 2003;36:1626.
[23] Murthy NS, Bray RG, Correale ST, Moore RAF. Polymer 1995;(36):3863.
[24] Ramesh C, Gowd EB. Macromolecules 2001;34:3308.
[25] Murthy NS, Minor H, Bednarczyk C, Krimm S. Macromolecules 1993;26:1712.
[26] Zhang Q-X, Fu P-P, Zhang H-F, Mo Z-S. Chem Res Chinese Uni 2002;18:358.
[27] Murthy NS. Text Res J 1997;677:511.
[28] Matyi RJ, Crist B. J Polym Sci, Polym Phys Ed 1978;16:1329.
[29] King SM. Ropes used underground are far more likely to be used wet, and are far more likely to pick up significant surface contamination (clay particles) that may necessitate mechanical washing (with or without detergent). On the other hand, UV exposure is negligible. Ropes used in climbing/mountaineering are normally used dry, pick up relatively little surface contamination, but are subject to extensive UV irradiation.
[30] Khanna YP, Kuhn WP. J Polym Sci, Polym Phys Ed 1997;35:2219.
[31] Sichina WJ, Cassel RB. Thermal Analysis Technical Report PETech-33. Perkin–Elmer Instruments; 2000.